THE JOURNAL OF BIOLOGICAL CHEMISTRY
Vol. 280, No. 20, Issue of May 20, pp. 20010–20020, 2005
Printed in U.S.A.

An Insulin-response Element-binding Protein That Ameliorates Hyperglycemia in Diabetes*[S]

Received for publication, September 20, 2004, and in revised form, March 4, 2005
Published, JBC Papers in Press, March 7, 2005, DOI 10.1074/jbc.M410817200

Betty C. Villafuerte‡§ and Elizabeth N. Kaytor¶‖

From the ‡Department of Medicine, University of Louisville School of Medicine, Louisville, Kentucky 40202 and the ¶Department of Medicine, Emory University School of Medicine, Atlanta, Georgia 30322

Insulin modulates glucose homeostasis, but the role of insulin-responsive transcription factors in such actions is not well understood. Recently, we have identified the insulin-response element-binding protein-1 (IRE-BP1) as a transcription factor that appears to mediate insulin action on multiple target genes. To examine the possibility that IRE-BP1 is an insulin-responsive glucoregulatory factor involved in the metabolic actions of insulin, we investigated the effect of adenoviral overexpression of hepatic IRE-BP1 on the glycemic control of insulin-resistant diabetic rats. Adenoviral IRE-BP1 lowered both fasting and postprandial glucose levels, and microarray of hepatic RNA revealed modulation of the expression of genes involved in gluconeogenesis, lipogenesis, and fatty acid oxidation. The insulin mimetic effects of IRE-BP1 were also confirmed in L6 myocytes; stable constitutive expressions of IRE-BP1 enhanced glucose transporter expression, glucose uptake, and glycogen accumulation in these cells. These findings showed physiologic sufficiency of IRE-BP1 as the transcriptional mediator of the metabolic action of insulin. Understanding IRE-BP1 action should constitute a useful probe into the mechanisms of metabolic regulation and an important target to develop therapeutic agents that mimic or enhance insulin action.

The prevalence of type 2 diabetes mellitus has increased substantially over the past decade, but the pathophysiological mechanisms for the development of the disease remain poorly understood (1). Current evidence indicates that major factors contributing to the pathogenesis of diabetes include decreased insulin effects on target tissues, increased endogenous glucose production, and elevated circulating free fatty acids and lipid oxidation (2–4). In the liver, insulin acts to suppress transcription of genes encoding gluconeogenic and glycogenolytic enzymes and stimulates transcription of genes encoding glycolytic and lipogenic enzymes, resulting in decreased glucose (5, 6). In patients with type 2 diabetes, the rate of hepatic gluconeogenesis is increased compared with control subjects, and hepatic resistance to the actions of insulin has been suggested to contribute to the development of fasting hyperglycemia, but the mechanism for impaired suppression of gluconeogenesis remains unknown (7, 8). Therefore, understanding the mechanism(s) by which insulin transduces its effects on hepatic glucose production may contribute to our understanding of the pathogenesis of diabetes.

Insulin stimulates gene transcription through both the mitogen-activated protein kinase and the phosphatidylinositol 3-kinase/protein kinase B (Akt) pathways (9, 10). Many studies have concluded that insulin-induced signals through the phosphatidylinositol 3-kinase-Akt pathway play a significant role in the metabolic actions of insulin, and Akt has been proposed to link insulin receptor binding to the activities of various insulin-responsive genes (11, 12). Recently, the forkhead transcription factor Foxo 01 was found to be phosphorylated by Akt and to control glucose homeostasis *in vivo*. Haploinsufficiency of *Foxo 01* was found to normalize blood glucose in an insulin-resistant mouse model and expression of a mutant cDNA that is resistant to inactivation by insulin-elevated fasting blood glucose levels (13, 14). Therefore, Foxo 01 may be a negative regulator of insulin action, but the transcription factor(s) that mediates the positive actions of insulin on glucose control has not been identified.

This laboratory recently identified a novel transcription factor that binds directly to the insulin-responsive elements of multiple genes, including the insulin-like growth factor-1 (*IGF-1*),[1] IGF-binding protein-3 (*IGFBP-3*), and *IGFBP-1* genes (15). The transcription factor insulin-response element-binding protein-1 (IRE-BP1) appears to be an Akt substrate, because it is phosphorylated by Akt *in vivo* and *in vitro*. Changes in expression level, phosphorylation, and nuclear translocation modulate the transactivation effects of the factor on the insulin-responsive element reporter genes. The level of expression of IRE-BP1 is decreased in insulin-deficient diabetes. Although the *IGFBP-3* gene, which was the basis for cloning of *IRE-BP1*, is known to be regulated by insulin, it has no established connection to the metabolic actions of insulin. To begin to study the biological effects of IRE-BP1, we established stable cell lines that express IRE-BP1 in L6 myocytes, and we examined the cells for metabolic changes relevant to insulin action. To determine whether expression of IRE-BP1 affects glucose control *in vivo*, we used recombinant adenovirus to express IRE-

* This work was supported by EmTech Biotechnology Development Inc., Georgia Institute of Technology Faculty Research Commercialization Program, and by the Walter F. and Avis Jacobs Foundation (to B. C. V.). The costs of publication of this article were defrayed in part by the payment of page charges. This article must therefore be hereby marked "*advertisement*" in accordance with 18 U.S.C. Section 1734 solely to indicate this fact.

[S] The on-line version of this article (available at http://www.jbc.org) contains Supplement A.

§ To whom correspondence should be addressed: Dept. of Medicine, Division of Endocrinology, University of Louisville School of Medicine, 570 S. Preston St., Donald Baxter Bldg., Rm. 221E, Louisville, KY 40202. Tel.: 502-852-4048; Fax: 502-852-2492; E-mail: bcvill01@louisville.edu.

‖ Present address: Fish & Richardson PC, 60 South 6th St., 3300 Dain Rauscher Plaza, Minneapolis, MN 55402.

[1] The abbreviations used are: IGF-1, insulin-like growth factor-1; IRE-BP1, insulin-response element-binding protein-1; PEPCK, phosphoenolpyruvate carboxykinase; ZDF, Zucker diabetic fatty; MES, 4-morpholineethanesulfonic acid; GTT, glucose tolerance test; GFP, green fluorescent protein.

BP1 in diabetic rats, and we assessed for changes in glucose homeostasis. We also used microarray of hepatic RNA to identify genes that are targeted by IRE-BP1. Our study shows that IRE-BP1 enhances some of the metabolic effects of insulin, including glucose uptake, glucose transporter expression, and glycogen accumulation in L6 myocytes. Overexpression of IRE-BP1 in the liver reduced both fasting and postprandial glucose levels in Zucker diabetic rats, probably through a mechanism that involves decreased hepatic gluconeogenesis, increased lipogenesis, and decreased lipid oxidation. Thus, we propose that IRE-BP1 may mediate some of the positive actions of insulin involved in lowering blood glucose levels, and we speculate that IRE-BP1 may be involved in the pathogenesis of diabetes.

EXPERIMENTAL PROCEDURES

Plasmid Construction and Stable Cell Line Expression of IRE-BP1—A 1503-bp fragment (+1641/+3144) of rat IRE-BP1 cDNA was inserted into the pCMV-tag2 vector (Stratagene, La Jolla, CA) at the SmaI site. Stable transfections were achieved with Targefect F2 and Virofect enhancer (Targeting Systems, San Diego); 60-mm dishes of L6 cells at 90% confluence were transfected with 6 μg of the IRE-BP1/pCMV-Tag2B construct or the empty vector overnight, followed by 48 h of recovery in fresh media. After the recovery period, G418 (Invitrogen) was added at 800 μg/ml for 14 days, when colonies were picked and expanded under G418 selection.

Measurement of Glucose Uptake—L6 cells were serum-starved in Dulbecco's modified Eagle's medium overnight at 37 °C and glucose-starved for 4 h before studies were conducted. Cells were stimulated with or without insulin (10 nM) for 15 min at 37 °C, followed by addition of 2-deoxy-[^{3}H]glucose (ICN, Costa Mesa, CA) at 2.8 μCi/ml in HBS buffer for 10 min. The plates were then washed to remove excess labeled glucose and lysed with 0.2 N NaOH (16). The samples were counted in a scintillation counter. Protein concentration was determined by the Bradford assay, and the data are expressed as deoxyglucose uptake (cpm)/μg protein.

Glycogen Content of the Cells—To stain for glycogen, L6 cells were oxidized with 0.5% periodic acid for 5 min, washed with water, and incubated with Schiff's reagent for 15 min. The cells were then rinsed with 10% sodium metabisulfite solution, and counterstained with Gill's hematoxylin solution for 30 s (17). To quantitate the glycogen content, a combined amyloglucosidase/glucose hexokinase assay was performed.

Quantitative PCR—The optimal primer pairs for amplification of IRE-BP1 cDNA (forward primer, 5′-GGGACCCACTTGTGAATCAG-3′; reverse primer, 5′-TTTCCAACCAGGTCAACACA-3′) were designed. The 5′-end of the 5′-primer was modified with addition of the T7 promoter and with an oligo(dT) at the 5′-end of the 3′-primer, as described by Totzke *et al.* (18). PCR products were amplified with the modified primer pairs, quantitated spectrophotometrically at 260 nm, and used for *in vitro* transcription with T7 RNA polymerase to produce IRE-BP1 cRNA, as described by Fronhoffs *et al.* (19). Reactions provided a DNA fragment of 197 bp. A standard curve of known amounts of IRE-BP1 cRNA was constructed by log dilutions of the *in vitro* transcription reaction product and converted to molecule number. Liver RNA was collected from 12-week-old lean, obese, and diabetic Zucker rats and from *ad libitum* fed and 3-day fasted Sprague-Dawley rats (n = 2–3 per group). The total RNA (5 μg) was reverse-transcribed into cDNA in parallel with the cRNA (10^{11} to 10^4 molecules) in the standard curve, and the cDNAs were then used for real time PCRs using SIBYL green incorporation for detection of the amplified products (Stratagene MX4000, La Jolla, CA). The number of molecules of IRE-BP1 mRNA was determined by plotting the amplified signals of the samples against signals produced by the coamplified standard mRNAs. Unknowns were quantitated by the threshold cycle number where the fluorescent signals were detected. Semi-quantitative RT-PCR analysis was performed utilizing primers designed to identify 13 S ribosomes to confirm equal loading of RNA.

Generation of Recombinant Adenovirus—Using the AdEasy system (Qbiogene, Inc.), the +1641 to +3144 fragment of rat IRE-BP1 cDNA was cloned into a shuttle vector (pShuttle-CMV). Once constructed, the shuttle vector was linearized with Pme1 and cotransformed into BJ5183 together with AdEasy-1, the supercoiled viral DNA plasmid. Transformants were selected for kanamycin resistance, and recombinants were subsequently identified by restriction digestion. Purified recombinant Ad plasmid DNA was digested with PacI to expose its inverted terminal repeats and then used to transfect AD-293 cells where deleted viral assembly genes are complemented *in vivo*. Recombinant adenovirus was obtained by plaque purification, amplified, and purified by Dr. Jude Samulski and co-workers at the University of North Carolina Vector Core Facility, Chapel Hill, NC. The adenovirus expressing IRE-BP1 was injected intravenously via the tail vein into Zucker diabetic rats, and the rats were monitored for blood glucose changes, as described under "Results."

Metabolic Studies—Serum glucose was measured using glucose oxidase strips. Rat insulin was measured with a radioimmunoassay kit from Linco Research in the Emory Endocrine Core Laboratory (inter-assay coefficient of variation = 0.20, intra-assay coefficient of variation = 0.06). To determine insulin sensitivity *in vivo*, insulin tolerance tests were conducted by administering a fixed bolus of regular insulin (2 units/kg body weight) intraperitoneally, and the decrease in plasma glucose was analyzed over the following 60 min. The slope of the linear decline in plasma glucose (K_{ITT}) was calculated by dividing 0.693 by plasma glucose half-time (50% from base line) using the following formula: $K_{ITT} = 0.693/t_{½} \times 100$, where $t_{½}$ represents the half-life of plasma glucose decrease (20) and ITT is insulin tolerance test. Normal K_{ITT} is >2.0%/min and values <1.5% are considered abnormal (Graph Pad Software, Inc., San Diego, CA). All animal studies were conducted with the approval of the Institutional Animal Care Committee of the Emory University and the University of Louisville.

Microarray Gene Analysis—To study the differential expression of genes expressed in rats treated with control vector or Ad IRE-BP1, we obtained hepatic RNA after overnight fasting from virus-treated rats 12 days after gene therapy. Six rat genome U34 GeneChip arrays (Affymetrix Inc., Santa Clara, California) consisting of 7,000 known genes and 1,000 ESTs, with ~16 pairs of oligonucleotide probes measuring the transcript level of each gene, were hybridized with hepatic tissue RNA obtained from three independent vector-treated and three Ad IRE-BP1-treated rats. Superscript II reverse transcriptase (Invitrogen) was used to synthesize the cDNA from total RNA (20 μg/sample). Biotin-labeled antisense cRNA was synthesized from the cDNA by *in vitro* transcription (BioArray high yield RNA transcript labeling kit, Enzo Life Sciences Inc., Farmingdale, NY) and hybridized initially with test chips to assess for hybridization background and sample quality, including determination of the hybridization ratio of the 3′-probe set to the 5′-probe set for actin and glyceraldehyde-3-phosphate dehydrogenase. Hybridization was performed with 10 μg of cRNA per GeneChip, and with 50 pmol of oligonucleotide B12, 0.1 mg/ml herring sperm DNA, 0.5 mg/ml acetylated bovine serum albumin in 100 mM MES, 1 M [Na^+], 20 mM EDTA, 0.01% Tween 20 at 45 °C for 16 h with mixing on a rotisserie at 60 rpm, then washed with 100 mM MES, 0.1 M [Na^+], 0.01% Tween 20. Controls for hybridization included known concentrations of *bio*B, *bio*C, *bio*D, and *cre* cRNAs. After washing with eukaryotic GE-WS2-V4 solution in Affymetrix Fluidics Station 400, probe arrays were scanned with an Agilent G2500A confocal laser scanner (Agilent Technologies, Palo Alto, CA). Expression signals were analyzed by using Affymetrix Microarray Suite 5.1 software and Datamining Tool version 3.0, scaled globally to a constant value, and data analysis generated detection p value and signal value, which assigned a relative measure of abundance to the transcript. Change in transcript expression when two arrays were compared, including the magnitude and direction of change, is expressed as signal log ratio and fold change. Cluster analysis was done using a Spearman correlation for similarity measures (Genespring version 6.0, Silicon Genetics) after normalization to the median of the control samples.

Statistical Methods—All values were expressed as the mean ± S.E. Experiments involving multiple sampling times, *i.e.* blood glucose and weight measurements over the 12-day study period, and the insulin tolerance test were analyzed with one-way analysis of variance using SigmaStat. For all other two-group comparisons, a nonpaired Student's t test was used. Differences were considered statistically significant at $p < 0.05$.

RESULTS

Biological Effects of IRE-BP1 in L6 Myoblasts—Using confocal microscopy, we previously showed that the NH_2-terminal segment of IRE-BP1 is localized to the cytoplasm, whereas the carboxyl segment is found predominantly in the nucleus of HepG2 cells (15). Furthermore, a 1.5-kb cDNA construct that encodes the 50-kDa carboxyl segment of IRE-BP1 transactivated the IGFBP-3 insulin-responsive element reporter gene, whereas addition of 5′-sequence to the cDNA attenuated the transcriptional activity of the expression vector, suggesting that IRE-BP1 is proteolyzed and that its carboxyl segment may

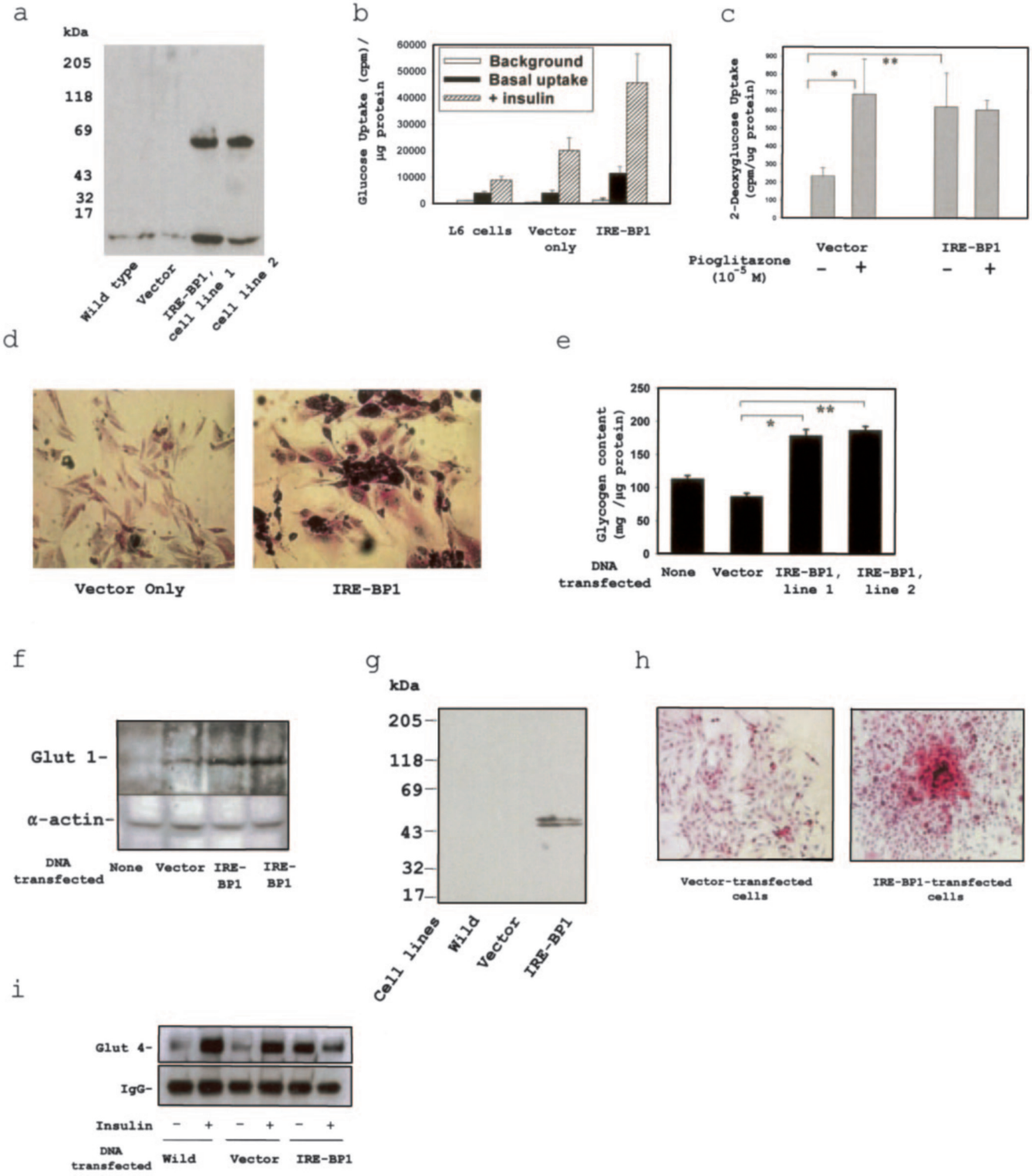

FIG. 1. **Biological effects of IRE-BP1 in L6 myocytes.** *a,* FLAG-tagged 1.5-kb IRE-BP1 cDNA in pCMV-Tag2 and pCMV-Tag2 vector were transfected into L6 cells. G418-resistant clones were isolated, and the Western blot of lysates was compared with wild type and vector-transfected L6 cells using anti-FLAG antibody. *b,* 2.8 μM 2-[^{3}H]deoxyglucose was added to L6 cells with or without added insulin (10^{-8} M) for 10 min. Glucose uptake was compared between wild type L6 myocytes and cells stably transfected with either vector only or IRE-BP1 cDNA. This experiment was repeated three times. □, background; ■, basal uptake; ▨, insulin-induced uptake. $p < 0.05$ for vector-transfected cells *versus* IRE-BP1-transfected cells at basal level and for mock- and vector-transfected cells *versus* IRE-BP1-transfected cells with insulin induction. *c,* cells were exposed to pioglitazone (10^{-5} M) or vehicle (Me_2SO) overnight, and glucose uptake was compared between vector- and IRE-BP1-transfected cells as in *b*. Mean ± S.E., $n = 3$. $p < 0.05$ for vector-transfected cells without pioglitazone *versus* with pioglitazone (*), and for vector- *versus* IRE-BP1-transfected cells (**). *d,* light micrographs (×400) of G418-resistant L6 myoblasts transfected with pCMV-Tag2 vector alone or with pCMV-Tag2-IRE-BP1 cDNA. Cells were stained with periodic acid-Schiff base for glycogen, and nuclei were counterstained with Gill's hematoxylin. *e,* cells were subjected to acid hydrolysis, and glycogen was measured by amyloglucosidase-hexokinase assay. Results are expressed as mean ± S.E., $n = 3$ each. Experiments done two times with similar results. $p < 0.05$ for vector *versus* IRE-BP1-transfected cells, both *line 1* (*) and *line 2* (**). *f,* total lysates from mock-, vector-, and IRE-BP1-transfected L6 cells were subjected to Western blotting and probed with anti-Glut 1 and anti-α-actin antibodies. *g,* total lysates from mock-, vector-, and IRE-BP1-transfected cells were subjected to Western blotting and probed with the anti-Glut 4

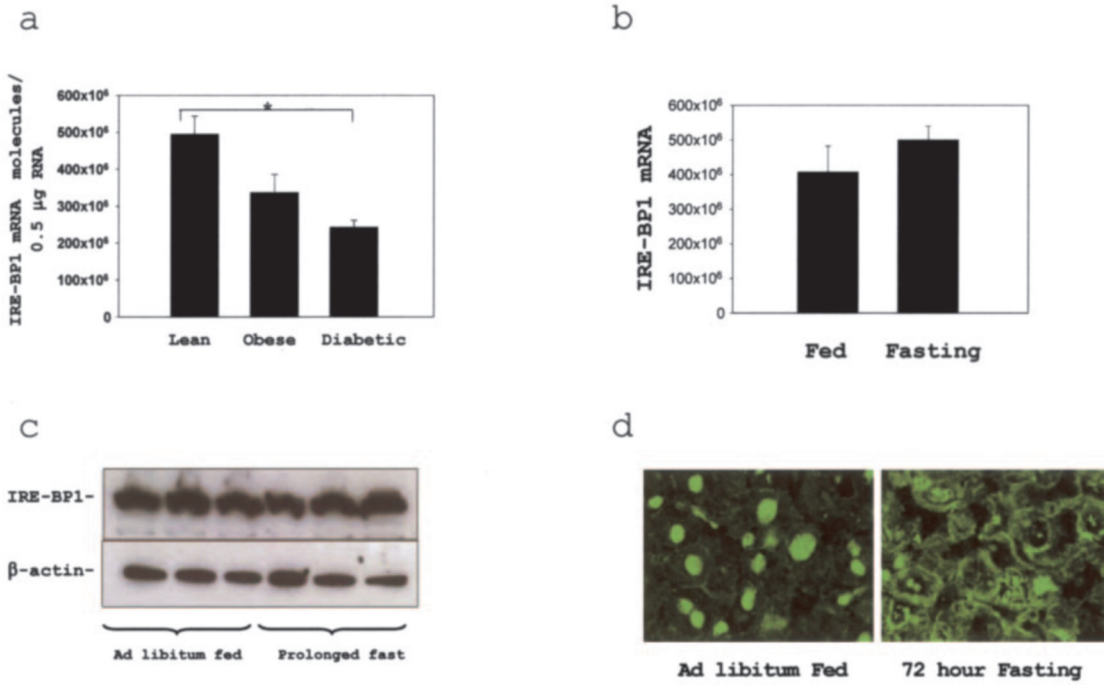

FIG. 2. **Regulation of hepatic IRE-BP1 *in vivo*.** *a,* the PCR-amplified products from liver RNA samples of lean, obese, and diabetic rats were plotted against the standard curve from known concentrations of IRE-BP1 cDNA, and the number of molecules of IRE-BP1 mRNA within the total isolated RNA preparations were determined. *, $p < 0.05$ for lean *versus* diabetic liver. Mean ± S.E., $n = 4$. *b,* IRE-BP1 mRNA was determined in the livers from *ad libitum* fed and 72-h fasted rats. Mean ± S.E. $n = 3$/group. $p = 0.47$ for fasted *versus* fed. *c,* cell extracts (50 µg/lane) from 72-h fasted and *ad libitum* fed animal livers were subjected to Western blotting and probed with IRE-BP1 carboxyl-specific and β-actin antibodies. *d,* confocal microscope image of liver section from fasted and fed animals, immunostained with IRE-BP1 carboxyl antibody. Magnification, ×1000.

translocate to the nucleus to bind and transactivate insulin-responsive sequences (15). Therefore, in this investigation and throughout the studies shown here, we used the 1.5-kb carboxyl segment of the cDNA to examine the biological consequences of IRE-BP1 expression.

Initially, the 1.5-kb cDNA was subcloned into pCMV-Tag2 to obtain an 8-amino acid "FLAG" tag at the N terminus (Stratagene, La Jolla, CA), and stable transfectants were produced in L6 myocytes. As shown in Fig. 1*a*, cell lysates from transfected cells expressed immunoreactive IRE-BP1 as a −70-kDa protein as detected by anti-FLAG antibody; the increase in size above the expected 50 kDa may reflect post-translational modifications. Uptake of 2-[^{3}H]deoxyglucose was increased −3-fold in the IRE-BP1-overexpressing cell line, compared with vector-transfected or wild type cells (Fig. 1*b*). After addition of 10^{-8} M insulin for 10 min, there was a 2- and 5-fold increase in glucose uptake in vector- and IRE-BP1-transfected cells compared with wild type cells, suggesting that IRE-BP1 may confer insulin-mimetic enhancement of glucose uptake. We also compared the effects of IRE-BP1 to those of pioglitazone, a thiazolidinedione used to increase insulin sensitivity and lower glucose levels in patients with diabetes. As shown in Fig. 1*c*, 2-[^{3}H]deoxyglucose uptake rose ~3-fold in wild type cells treated with pioglitazone for 16 h, consistent with previous reports (21, 22), and was comparable with glucose uptake in IRE-BP1-overexpressing cells. However, the addition of pioglitazone produced no further increase in glucose uptake in the IRE-BP1-overexpressing cells, suggesting that IRE-BP1 may be sufficient to confer most of the stimulation of pioglitazone for glucose uptake.

Because insulin promotes glucose storage as well as glucose uptake *in vivo*, we used periodic acid-Schiff staining to evaluate the glycogen content of the transfected cells. As shown in Fig. 1*d*, IRE-BP1-overexpressing L6 cells exhibited much higher glycogen content than vector-transfected cells, with an accompanying change in morphology from a predominantly spindle shape to a more cuboidal shape in association with expansion of the cytoplasm. Compared with vector-transfected cells, IRE-BP1 overexpression increased glycogen content of the two cell lines by 106 ± 10 and by 115 ± 7%, as measured by the amyloglucosidase-hexokinase assays (both $p < 0.05$ *versus* vector control, Fig. 1*e*).

To explore the mechanisms underlying the impact of IRE-BP1 on glucose uptake, glucose transporter expression was examined. As shown in the immunoblot in Fig. 1*f*, wild type L6 or vector-overexpressing cells contain low levels of the Glut 1 transporter, but the IRE-BP1-overexpressing cells exhibited a 3-fold increase in Glut 1 compared with vector-transfected cells. In addition, although the Glut 4 transporter that is the major effector of glucose transport in skeletal muscle is often expressed at a low level in muscle cell lines in the absence of insulin (23), Glut 4 was detected even without added insulin in IRE-BP1-transfected cells (Fig. 1*g*). Moreover, the Glut 4 antibody provided no significant reaction with vector-transfected cells, although immunostaining was strongly positive in IRE-BP1-overexpressing cells (Fig. 1*h*). To investigate further the relationship between IRE-BP1 and insulin action in stimulating Glut 4, we immunoprecipitated Glut 4 from cells grown in the presence or absence of insulin. As shown in Fig. 1*i*, Glut 4 expression was low in both the mock- and vector-transfected cells but was high in IRE-BP1-transfected cells. When 10^{-8} M insulin was added for 48 h, Glut 4 was significantly stimulated in mock- and vector-transfected cells but was not stimulated

antibody. *h,* immunostain of vector-transfected and IRE-BP1-transfected cells with anti-glut 4 antibody. Color reaction developed with ABC-Vector red complex from alkaline phosphatase kit (Vector Laboratories). *i,* total lysates from mock-, vector-, and IRE-BP1-transfected L6 cells treated with or without insulin (10^{-8} M) for 48 h were immunoprecipitated with anti-Glut 4 antibody, followed by Western blotting with the same antibody. The blot was reprobed with anti-rabbit IgG to show equal loading of the proteins.

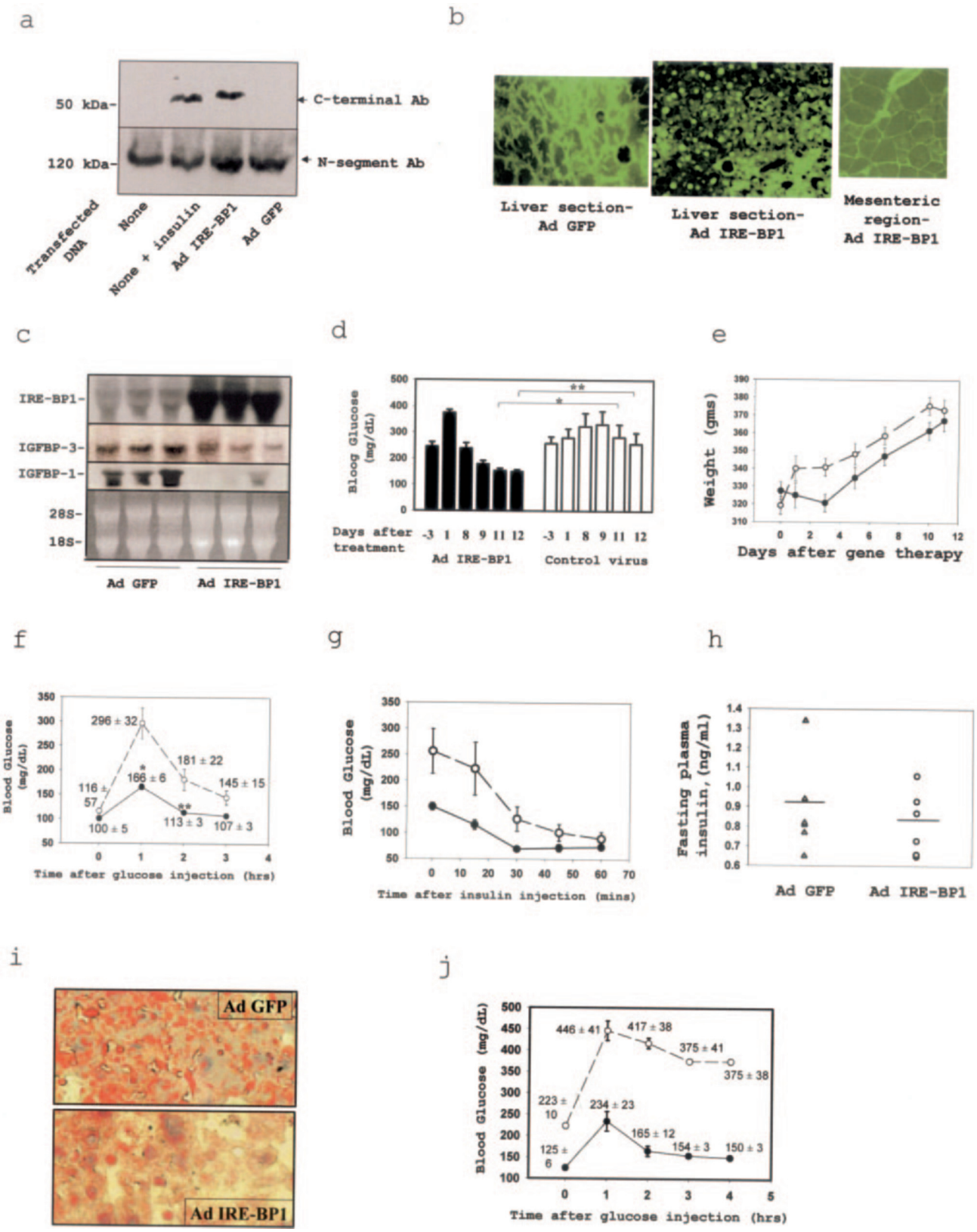

FIG. 3. **Effects of IRE-BP1 on glucose control in diabetic rats.** *a,* recombinant adenovirus encoding IRE-BP1 or GFP was transfected into 3T3-L1 adipocytes at 100 plaque-forming units/cell. After 48 h, cell lysates were subjected to Western blot analysis and probed with IRE-BP1 antibodies (carboxyl-specific and NH_2 segment-specific antibody (*Ab*)). *b,* microscopic sections of liver and mesenteric fat from Ad IRE-BP1- and Ad GFP-treated rats. Tissues were embedded in optimum cutting temperature compound, cut into 0.4-mm sections, and visualized directly with an immunofluorescent microscope. Magnification ×400. *c,* Northern blot analysis of hepatic tissues obtained from Ad GFP- or Ad IRE-BP1-treated rats (100 μg of RNA/lane), probed with IRE-BP1, IGFBP-3, and IGFBP-1 cDNA probes. *d,* glucose was measured in blood samples obtained from the tail vein of Ad IRE-BP1-treated ($n = 6$, *black bars*) and Ad GFP-treated ($n = 6$, *white bars*) *ZDF* rats before and after gene therapy as indicated. Values are mean ± S.E. The experiment was repeated in three different sets of animals with similar results. $p < 0.05$ for IRE-BP1 *versus* control virus treatments on days 11 (*) and 12 (**). *e,* body weights before and after gene therapy. Values are mean ± S.E., $n = 6$ per group. The *solid circle*

further in IRE-BP1-transfected cells; a decrease in Glut 4 with addition of insulin may be related to a sample loading problem, because the control IgG was also lower. This result suggests that IRE-BP1 may be sufficient to increase Glut 4 expression or that IRE-BP1 may mediate insulin stimulation of Glut 4, because insulin provided no additional effect in the presence of IRE-BP1 overexpression. Together, these findings show that IRE-BP1 increased glucose transporter expression, glucose uptake, and glycogen storage, the biological processes that mimic insulin action. The effect of IRE-BP1 appears not to be related to differentiation of the myogenic cell line, because two of the helix-loop-helix proteins (myoD and myogenin) known to regulate muscle cell development were not significantly affected; and furthermore, induction of L6 myocytes to myotubes did not affect the biological activity induced by IRE-BP1 (data not shown).

Regulation of Hepatic IRE-BP1 in Vivo—We have shown previously that hepatic IRE-BP1 mRNA is decreased in streptozotocin-diabetic rats compared with normal rats (15). To determine whether a similar decrease in IRE-BP1 expression occurs in type 2 diabetes, we compared the hepatic expression of IRE-BP1 in Zucker diabetic rats to that of lean and obese non-diabetic Zucker rats. The Zucker diabetic fatty (ZDF)-*drt* rat expresses mutant forms of the leptin receptor and is a model of obesity complicated by diabetes (24). In this experiment, we designed primers that amplified a 197-bp region of IRE-BP1 cDNA, and we used real time PCR to measure the mRNA expression of IRE-BP1. Our studies show that liver from 12-week-old diabetic rats have 51 ± 3% lower expression of IRE-BP1 mRNA than age-matched lean controls ($p = 0.027$ *versus* control, Fig. 2*a*). There was also a 32 ± 9% decrease in IRE-BP1 expression in obese rats ($p = 0.08$ *versus* control), suggesting that insulin resistance in obesity as well as type 2 diabetes is associated with decreased hepatic IRE-BP1 expression.

Because fasting affects the regulation of hepatic enzymes involved in maintaining the blood glucose level, we also determined whether hepatic IRE-BP1 expression was affected in the transition from fasting to feeding. We obtained livers from Sprague-Dawley rats that were fed *ad libitum* or subjected to 72 h of fasting, and we found no significant change in the expression of IRE-BP1 ($p = 0.47$ for fed *versus* fasting, Fig. 2*b*). No change in IRE-BP1 was also found after 48 h of fasting (data not shown). To determine whether fasting affects the protein translation of IRE-BP1, we obtained total liver extracts and assessed for changes in the IRE-BP1 protein. As shown by Western blotting in Fig. 2*c*, compared with fed animals, there was no significant change in the IRE-BP1 protein levels with prolonged fasting. Because nuclear translocation of IRE-BP1 affected its transactivation activity, we also prepared tissue sections from rat liver, and we determined the cellular localization of the protein. As shown in Fig. 2*d*, there was a dramatic change in the cellular localization of IRE-BP1 with prolonged fasting, as detected by an antibody that recognized the carboxyl segment of the protein. During normal feeding, confocal microscopy showed that IRE-BP1 was localized predominantly to the nuclei of hepatocytes. With prolonged fasting, however, IRE-BP1 was localized mainly to the cytoplasm. Therefore, there is either decreased nuclear translocation of the protein, or the protein is exported from the nucleus with fasting. In either case, the transcriptional program stimulated by IRE-BP1 will be expected to be low in fasted animals.

In Vivo Effects of IRE-BP1 in Diabetes—Because our previous study showed that proteolysis of IRE-BP1 affects its transcriptional activity, the physiologic function of IRE-BP1 was tested further by determining whether the truncated IRE-BP1 had insulin-like effects *in vivo*. In this experiment, we constructed an adenoviral vector containing the transcriptionally active fragment of IRE-BP1 (+1641/+3144), and we confirmed that the recombinant virus (Ad IRE-BP1) increased expression of ~50-kDa IRE-BP1 in 3T3-L1 adipocytes (Fig. 3*a*). The adenoviral constructs at a dose of 5.0×10^7 plaque-forming units/g body weight were introduced via tail vein infusion into 10-week-old male Zucker diabetic fatty (*ZDF*) rats. Controls included age-matched *ZDF* rats infused with virus encoding the green fluorescent protein (Ad GFP) at a dose equivalent to that of Ad IRE-BP1. Because we used a fusion construct of GFP and IRE-BP1, we were able to track the tissue distribution of the autofluorescent protein after administration. Tissue sections showed high expression of Ad IRE-BP1 in the liver, particularly in hepatocyte nuclei, and also high expression in mesenteric adipocytes and mesenteric veins (Fig. 3*b*), whereas Ad GFP was localized mainly to the hepatic sinusoidal area. There was no significant fluorescent signal detected in either the pancreas or skeletal muscles (data not shown). Northern blotting showed that hepatic IRE-BP1 was increased by administration of the transgene (Fig. 3*c*). Preliminary studies showed no difference between vehicle or Ad GFP (viral vector) infusions in glucose levels in the *ZDF* rats, and that the effects of Ad IRE-BP1 were similar whether the adenovirus was introduced via the portal vein or tail vein.

Before treatment, base-line glucose levels in *ad libitum* fed Ad IRE-BP1- and Ad GFP-treated rats ($n = 6$ per group) were not significantly different (245 ± 17 *versus* 258 ± 25 mg/dl; Fig. 3*d*). There was a transient increase in plasma glucose 24 h after administration of Ad IRE-BP1, followed by a gradual decline over 10–12 days. Compared with base line, there was a significant decrease in the glucose levels of IRE-BP1-treated rats at 12 days (245 ± 17 *versus* 151 ± 9 mg/dl, $p < 0.05$). In contrast, glucose levels remained high in GFP-treated rats (base line of 258 ± 25 *versus* 282 ± 48 mg/dl at 12 days, $p =$ not significant). Body weights increased in parallel in both groups and were not significantly different between the two groups at the end of the study (367 ± 6 *versus* 373 ± 8 g for IRE-BP1-treated and control rats, respectively, Fig. 3*e*).

On day 11, both groups of animals were fasted overnight (16 h) and had a glucose tolerance test (GTT) with intraperitoneal injection of 50% dextrose at 2 g/kg body weight (Fig. 3*f*). Tail vein fasting glucose levels were slightly lower in IRE-BP1-treated compared with GFP-treated rats (101 ± 5 *versus* 116 ± 6 mg/dl), but the difference was not significant. During the GTT, glucose levels were significantly lower in the IRE-BP1-

represents Ad IRE-BP1-treated and the *open circle* represents Ad GFP-treated rats. *f,* glucose tolerance test. After overnight fast, 2 g of dextrose/kilogram body weight was injected intraperitoneally into Ad IRE-BP1- and Ad GFP-treated rats, and blood glucose was measured every hour for 3 h. The *solid circles* represent Ad IRE-BP1 and the *open circles* represent data from Ad GFP-treated rats. Mean ± S.E., $n = 6$ each. $p < 0.05$ for IRE-BP1 *versus* control virus treatment at 1 (*) and 2 h (**) post-injection. *g,* insulin tolerance test. Insulin was injected at 2 units/kg intraperitoneally, and the blood glucose was measured every 15 min in Ad IRE-BP1- (●) and Ad GFP (○)-treated rats. $p < 0.05$ for Ad GFP *versus* Ad IRE-BP1 treatment at base line and 15 min after injection of insulin. *h,* fasting plasma insulin levels of Ad GFP (△) and Ad IRE-BP1-treated rats (○) 12 days post-therapy. *Horizontal line* indicates the mean value. $p = 0.6$ for the two treatments, $n = 6$/group. *i,* liver sections from Ad GFP and Ad IRE-BP1-treated rats were stain with Oil Red O for lipoid deposits. Similar pattern was observed in the livers of three Ad GFP and three Ad IRE-BP1 treated rats. *j,* GTT was repeated in 18-week-old *ZDF* rats as in *f*. The results are shown in *solid line* for Ad IRE-BP1-treated ($n = 3$) and *broken line* for Ad GFP-treated rats ($n = 4$). Each *number* represents mean ± S.E. $p < 0.05$ for Ad GFP *versus* Ad IRE-BP1 treatments for all the time periods examined.

treated rats than control, with values of 166 ± 6 at 1 h and 113 ± 3 mg/dl at 2 h, compared with glucose levels in the GFP-treated rats of 296 ± 31 and 181 ± 22 mg/dl. This result revealed improved glucose tolerance in IRE-BP1-treated rats. After the GTT, the rats were fasted for an additional 6 h, and an insulin tolerance test was conducted. Regular insulin at 2 units/kg body weight was given intraperitoneally, and plasma glucose levels was measured over a 60-min period by tail vein sampling. As shown in Fig. 3*g*, glucose levels in the Ad IRE-BP1-treated rats decreased from 150 ± 7 to 115 ± 9, 69 ± 5, 72 ± 7, and 74 ± 5 mg/dl at 15, 30, 45, and 60 min after administration of insulin, whereas glucose levels in Ad GFP-treated rats decreased from 256 ± 43 to 223 ± 51, 126 ± 22, 101 ± 16, and 89 ± 13 mg/dl, respectively ($p < 0.001$ by analysis of variance). The slope of the decline in plasma glucose (K_{ITT}) was calculated to be 4.8%/min in IRE-BP1-treated rats and 1.59%/min in GFP-treated rats, and the half-life of plasma glucose decrease was 14 min in IRE-BP1-treated rats and 35 min in GFP-treated rats. These findings are consistent with increased insulin sensitivity with IRE-BP1 expression. On day 12, the rats were fasted overnight and sacrificed, and hepatic tissues were collected for measurement of glycogen and analysis of gene expression. Mean fasting insulin levels were similar in IRE-BP1-treated and GFP-treated rats (0.81 ± 0.06 *versus* 0.91 ± 0.12 ng/ml, $p = 0.5$, Fig. 3*h*), whereas the liver glycogen content (61 ± 13 *versus* 50 ± 9 nmol/mg) was slightly higher; these findings are again consistent with increased insulin sensitivity. Because hepatic steatosis is associated with insulin resistance, we used Oil Red O stain to evaluate for fat deposits in the liver section of the animals under fasting condition. As shown in Fig. 3*i*, IRE-BP1-treated livers appear to have a significant decrease in fat droplet contents compared with vector-treated livers. This change was consistent with the gross appearance of the livers, in which the yellow discoloration of the liver was reduced significantly with IRE-BP1 treatment (not shown).

In a separate experiment, we performed a GTT in 18-week-old *ZDF* rats with more severe diabetes. By this age, linear growth has ceased, and hyperglycemia can be assessed independent of weight gain from growth. Before gene therapy, glucose levels during *ad libitum* feeding were 395 ± 18 mg/dl in IRE-BP1-treated and 390 ± 18 mg/dl in GFP-treated rats. Fourteen days after therapy, despite comparable body weights (435 ± 8 g in IRE-BP1- and 421 ± 14 g in GFP-treated rats), the fasting glucose level was significantly lower in IRE-BP1-treated compared with GFP-treated rats (125 ± 6 mg/dl *versus* 223 ± 10 mg/dl, $p < 0.001$) (Fig. 3*j*). During the GTT, glucose levels in the IRE-BP1-treated rats rose to 165 ± 12 and 150 ± 3 mg/dl at 2 and 4 h post-challenge, whereas glucose levels in the GFP-treated rats were 417 ± 38 and 375 ± 38 mg/dl (both $p < 0.05$ *versus* values in IRE-BP1-treated animals). Our findings demonstrate that overexpression of IRE-BP1 decreases fasting glucose and improves the response to a glucose challenge. Treatment with IRE-BP1 therefore appears to be sufficient to ameliorate hyperglycemia in *ZDF* rats.

Genes Targeted by IRE-BP1 as Determined by DNA Microarray Analysis—To understand the mechanism by which hepatic expression of IRE-BP1 improves the plasma glucose concentrations, microarray analysis was used to compare the level of expression of hepatic mRNAs in *ZDF* rats treated with Ad GFP or Ad IRE-BP1. To minimize individual animal differences, and to eliminate effects secondary to differing plasma glucose and insulin levels, messenger RNA expression was studied in 12-week-old rats under fasting conditions 12 days after gene therapy. Tissues were harvested from animals with fasting glucose levels of 105 ± 5 and 100 ± 1 mg/dl and insulin levels of 0.79 ± 0.1 and 0.85 ± 0.04 ng/ml with IRE-BP1 and GFP treatments, respectively. The relative level of gene expression was compared by performing pairwise comparisons between independent microarrays from three GFP-treated rats and three IRE-BP1-treated rats, giving nine cross-comparison replicates. When differences in expression level for a particular gene occurred consistently in the same direction compared with control values (Ad GFP-treated), the average fold change in mRNA expression was calculated, and the values with p value less than 0.003 by Wilcoxon's signal rank test were considered significant and were included in the analysis.

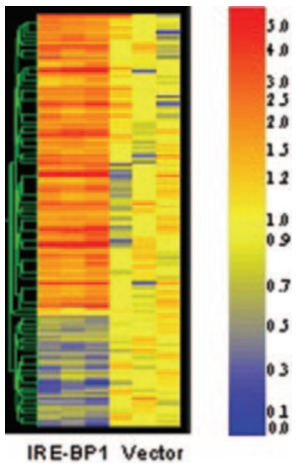

FIG. 4. **Genes that are increased or decreased by IRE-BP1 treatment in hepatic tissue.** Cluster analysis showing relative RNA message levels for genes that were up-regulated (*red-shifted*) or down-regulated (*blue-shifted*) in Ad IRE-BP1-treated (*1st 3 lanes*) *versus* control hepatic tissues (*last 3 lanes*) of diabetic rats. Relative signal abundance is shown as IRE-BP1-treated over median of control samples for genes that increase or decrease at least ± 1.5-fold or greater. Data are coded according to the *red-blue color spectrum* depicted on the *right*. Specific genes regulated are listed in Supplement A.

By using Affymetrix RGU34A microchips containing 8,000 individual rat genes and ESTs, ~400 genes and ESTs (5.0%) were identified as altered with greater than 1.5-fold change in expression level. The magnitude of the changes ranged from 1.5- to 22-fold. Among these genes, 282 probe sets (70.5%) were found to be up-regulated, and 118 sets (29.5%) were down-regulated; expression of housekeeping genes (cyclophilin, β-actin, and ribosomal proteins) was comparable for vector- and IRE-BP1-treated hepatic tissues. Overexpression of IRE-BP1 was found to affect the expression of genes involved in fuel metabolism, electron transport, signal transduction, cell proliferation, and apoptosis. Fig. 4 shows a cluster analysis depicting relative changes in 146 genes with or without IRE-BP1 treatment. Relative expressions are depicted according to the color-code spectrum, with red shift signifying up-regulation and blue-shift signifying RNA message down-regulation (The complete list of the genes is included as Supplement A). Overexpression of IRE-BP1 altered the expression of a large number of genes involved in glucose and fatty acid homeostasis. Table I shows the genes that were increased significantly by IRE-BP1 expression in the rat liver compared with vector treatment. Among these were many genes whose products are required for lipogenesis, fatty acid transport/storage, cholesterol biosynthesis, cell signaling, and gene transcription. Notably, IRE-BP1 increased the expression of a significant number of genes that were reported previously to be stimulated by insulin, including lipoprotein lipase, fatty-acid synthase, thyroxine-binding globulin, transferrin receptor, and others (25); but the results also include a number of genes that were not implicated previ-

TABLE I
Genes up-regulated by IRE-BP1

Genes	Fold change (mean ± S.D.)
Triglyceride breakdown	
Stearyl-CoA desaturase	12.5 ± 1.6
Lipoprotein lipase	1.6 ± 1.2
Cholesterol biosynthesis/metabolism	
Hydroxymethylglutaryl-CoA reductase	3.3 ± 3.0
Cholesterol 7α-hydroxylase	2.9 ± 2.1
Squalene epoxidase	2.7 ± 1.4
3-Hydroxy-3-methylglutaryl-coenzyme A synthase	2.2 ± 1.2
Lanosterol 14-demethylase	2.0 ± 1.1
Farnesyl-diphosphate synthase	1.9 ± 1.6
Squalene synthetase	1.8 ± 1.2
7-Dehydrocholesterol reductase	1.7 ± 1.3
Fatty acid synthesis/transport/storage	
Fatty acid-binding protein 2	3.9 ± 1.6
Fatty-acid synthase	3.2 ± 1.9
Acetyl-CoA carboxylase	3.1 ± 1.7
Acyl carrier protein domain of fatty-acid synthase	2.5 ± 2.6
ATP-citrate-lyase	2.4 ± 1.6
Malic enzyme	1.9 ± 1.6
Intestinal fatty acid-binding protein	1.8 ± 1.2
Signaling molecules	
cAMP phosphodiesterase	8.4 ± 1.3
Phospholipase A (PS-PLA1)	4.2 ± 1.8
Casein kinase II β subunit (CK2)	1.9 ± 1.4
MEKK1	1.7 ± 1.3
LIMK-2a	1.6 ± 1.1
Purinergic receptor P2Y	1.6 ± 1.3
Extracellular signal-related kinase (ERK3)	1.5 ± 1.2
Protein kinase Cϵ	1.5 ± 1.1
Presenilin-2	1.5 ± 1.2
Protein phosphatase 2A, 55-kDa regulatory subunit α	1.5 ± 1.2
Transcription factors	
Angiotensin gene-inducible enhancer-binding protein 1	5.9 ± 1.7
Chromosomal protein HMG2	2.0 ± 1.5
Nuclear factor κB p105	1.8 ± 1.2
Nuclear oncoprotein p53	1.7 ± 1.2
APP-binding protein 1	1.6 ± 1.2
p21 (C-ki-ras)	1.5 ± 1.2
Others	
Adiponutrin	21.3 ± 3.4
DNA polymerase α	13.5 ± 1.7
Mdr p-glycoprotein	10.0 ± 1.3
Tsx or turn-on sex specificity	8.5 ± 1.3
Thyroxine-binding globulin	6.9 ± 2.7
Macrophage metalloelastase or MMP-12	6.7 ± 1.6
Cytochrome P450 4F5	6.0 ± 2.0
Insulin-induced growth response protein	2.5 ± 1.5
Transferrin receptor	2.3 ± 1.9
Apolipoprotein B editing protein	2.1 ± 1.2
GADD 45	1.7 ± 1.2
Apolipoprotein A-I	1.5 ± 1.5

ously to be insulin-regulated, such as modulators of cell cycle arrest and apoptosis (Bad and p53 oncogene), and genes that modulate inflammation (NF-κB p105, cytochrome p450 4F5). Table II shows the genes that were down-regulated. Among these were genes involved in gluconeogenesis and fatty acid oxidation. To begin to verify the data obtained from these experiments, we used Northern blot analysis to show that IGFBP-1 and IGFBP-3 expression are down-regulated by IRE-BP1 (Fig. 3*c*), as in the microarray analysis. Therefore, IRE-BP1 regulates transcription of regulatory enzymes involved in glucose and fuel metabolisms, consistent with an insulin mimetic action.

DISCUSSION

In vivo, the liver plays an important role in the regulation of fasting and postprandial glucose levels. Under fasting conditions, it releases glucose into the systemic circulation by mobilizing glycogen stores through glycogenolysis and by converting lactate, gluconeogenic glycerol, and amino acids into glucose through gluconeogenesis (9). Insulin is the most important hormone that inhibits gluconeogenesis (6). At the gene transcription level, insulin decreases the mRNAs encoding gluconeogenic enzymes such as phosphoenolpyruvate carboxykinase (PEPCK), which controls the rate-limiting steps of gluconeogenesis involving the conversion of pyruvate to glucose, and glucose-6-phosphatase, which regulates the terminal step common to gluconeogenesis and glycogenolysis before glucose is released from the liver (26, 27). Type 2 diabetes is characterized by the inability of insulin to down-regulate appropriately the activity of gluconeogenic enzymes, resulting in increased hepatic glucose output and elevated blood glucose levels (6). In this study, we found that systemic administration of recombinant IRE-BP1 induced high levels of IRE-BP1 expression in hepatocytes, which leads to improved glucose control in diabetic rats. To determine the mechanism by which IRE-BP1 decreased glucose level in diabetes, we analyzed the changes in hepatic gene expressions associated with overexpression of IRE-BP1. Our study showed that in diabetic rats, gene therapy with IRE-BP1 leads to down-regulation of PEPCK and glucose-6-phosphatase expression. Compared with control virus-treated hepatic tissue, we found a 2.7-fold de-

TABLE II
Genes down-regulated by IRE-BP1

Genes	Fold change (mean ± S.D.)
Gluconeogenesis/glycogenolysis/glucose uptake	
Glucose-6-phosphatase	−2.7 ± 1.4
Phosphoenoylpyruvate carboxykinase (PEPCK)	−1.6 ± 1.4
Glucokinase	−1.5 ± 1.5
Fatty acid oxidation	
Carnitine palmitoyltransferase 1	−1.7 ± 1.1
Dodecenoyl-CoA delta isomerase	−1.5 ± 1.2
Long chain acyl-CoA synthetase	−1.5 ± 1.2
Fatty acid-CoA ligase, long chain 2	−1.5 ± 1.1
Cholesterol esterase	−1.5 ± 1.4
Others	
IGFBP-1	−4.1 ± 2.0
Carbonic anhydrase III	−3.1 ± 1.3
Histidase	−2.6 ± 1.3
Diabetes-inducible cytochrome P450RLM6	−2.3 ± 1.3
Regucalcin	−2.3 ± 1.6
Hypoxia up-regulated 1	−2.2 ± 1.3
Epoxide hydrolase	−2.1 ± 1.2
Calcium-binding protein	−2.1 ± 1.4
Retinol dehydrogenase type II	−2.0 ± 1.5
IGFBP-3	−1.8 ± 1.3
Cystathione β-synthase	−1.8 ± 1.2
Carboxylesterase	−1.8 ± 1.1
IGFBP complex acid-labile subunit	−1.6 ± 1.2
IGF-1	−1.6 ± 1.1
Apolipoprotein C-IV	−1.6 ± 1.1
Apolipoprotein A-IV	−1.5 ± 1.2

crease in glucose-6-phosphatase and a 1.6-fold decrease in PEPCK mRNAs in IRE-BP1-treated liver. There was also a 1.5-fold decrease in expression of the gene encoding the glycolytic enzyme glucokinase (28). Although the tissues were obtained under fasting conditions, the effects on gene expression are similar to those observed in fed animals when insulin levels are high, indicating that the liver of IRE-BP1-treated rats is programmed to decrease glucose production, and expression of IRE-BP1 in the liver may mimic the effect of insulin to suppress gluconeogenesis. Consistent with this, we found that adiponutrin, a transmembrane protein previously reported to be elevated under fed conditions but decreased under fasting conditions, was increased 21-fold by IRE-BP1 overexpression (29, 30). Our study also showed that IRE-BP1 increased cAMP-specific phosphodiesterase 8.4-fold. Activation of this enzyme may counteract glucagon-induced production of cAMP, activation of glycogen phosphorylase, and decrease of hepatic glucose release (31–34). Concomitantly, cAMP-dependent protein kinase A activity could be reduced, leading to dephosphorylation and inactivation of hormone-sensitive lipase and reduced release of free fatty acids from hepatocytes (35), which may ameliorate insulin resistance in other insulin target tissues. Consistent with its ability to suppress gluconeogenesis, IRE-BP1 is regulated by prolonged fasting, a condition associated with stimulation of gluconeogenesis (36). During fasting, IRE-BP1 processing is impaired or is exported from the nucleus to the cytosol. Either mechanism serves to sequester IRE-BP1 from its target genes in the nucleus and prevent its transcriptional inhibition of gluconeogenic enzymes.

We found that IRE-BP1 expression also increased the mRNA level of a number of genes involved in fatty acid homeostasis. Among these were enzymes required for lipogenesis (fatty acid synthase), proteins of the malate cycle (malic enzyme), and an enzyme that catalyzes the conversion of citrate to acetyl-CoA in the cytosol (ATP-citrate-lyase) (37). In terms of the magnitude of change in expression, IRE-BP1 appears to markedly stimulate stearyl-CoA desaturase (12.5-fold), which is a protein involved in the synthesis of mono-unsaturated from saturated fatty acids, and is also necessary for triglyceride incorporation into very low density lipoprotein and low density lipoprotein cholesterol (38). A further decrease in triglyceride levels may be induced by the increased expression of lipoprotein lipase (39). Perhaps more importantly, genes involved in fatty acid oxidation are regulated by IRE-BP1. In the liver, mitochondrial fatty acid oxidation is controlled primarily by acetyl-CoA carboxylase-mediated modulation of intracellular malonyl-CoA levels (40). When acetyl-CoA carboxylase is activated, as in conditions associated with adequate glucose and insulin levels, malonyl-CoA is activated (40). Malonyl-CoA is an allosteric inhibitor of carnitine palmitoyltransferase 1 (CPT-1), the rate-limiting enzyme in fatty acid oxidation (41). Fatty acid oxidation provides ATP and reducing equivalents required for gluconeogenesis (42). β-Oxidation also produces intramitochondrial acetyl-CoA, which is essential for activation of pyruvate carboxylase, a key regulatory enzyme of gluconeogenesis (43). IRE-BP1 increased the expression of acetyl-CoA carboxylase by 3.1-fold and decreased the expression of CPT1 and long chain acyl-CoA synthetase by 1.7- and 1.5-folds, respectively. This pattern of expression may inhibit substrate flux through the fatty acid oxidation pathway and lead to further down-regulation of gluconeogenesis in the liver.

Based on the microarray analysis, IRE-BP1 appears to affect transcription of genes that are involved not only in hepatic gluconeogenesis and glycogenolysis but also in fat storage and fatty acid oxidation. Although lipogenic gene expression is increased and the expression of fatty acid oxidation genes is reduced, we found a paradoxical decrease in liver fat content with IRE-BP1 treatment. This may be due to an increase in triglyceride release from the liver, as suggested by changes in the expression of genes involved in lipid transport and very low density lipoprotein triglyceride production. Indeed, there is recent evidence that both intracellular and plasma free fatty acids and triglyceride levels play a significant role in amplifying the metabolic derangements of diabetes. By regulating a set of metabolic genes that decrease triglyceride levels and fatty acid oxidation, IRE-BP1 could potentially act to decrease insulin resistance through mechanisms that involve decreased release of free fatty acids into the circulation. This may improve postprandial glucose control by decreasing resistance to insulin

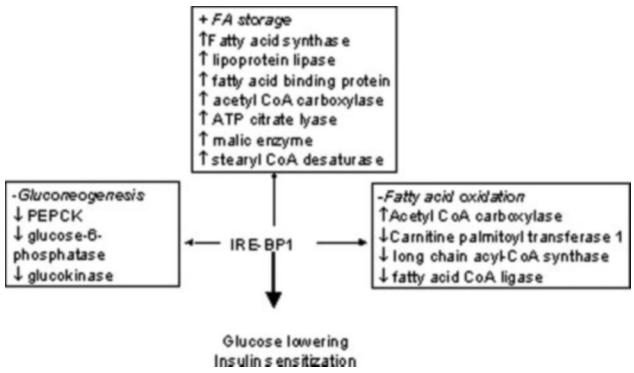

FIG. 5. **Model for the physiological actions of IRE-BP1.** IRE-BP1 either stimulates (+) or represses (−) key metabolic pathways in liver that decrease glucose production. Key genes regulated by IRE-BP1 are indicated. *FA,* fatty acid.

action in tissues other than the liver, including adipose tissue and skeletal muscle (44). Thus, the expression data reveal that hepatic IRE-BP1 has coordinate effects on at least three metabolic pathways involved in glucose metabolism: gluconeogenesis, lipogenesis, and fatty acid oxidation (Fig. 5). Our tissue expression analysis was conducted under fasting conditions, but because IRE-BP1 has a significant effect on postprandial glucose levels (shown in Fig. 3, *f* and *j*), it is likely that the magnitude of change in gene expression is amplified in tissues obtained under fed conditions. Although the administered viral vector localized mainly to hepatocytes, we cannot rule out an additional effect in adipose tissue, because the vector also localized to the mesenteric fat.

Consistent with its insulin mimetic action, IRE-BP1 decreased the expression of IGFBP-1 mRNA, which was reported previously to be negatively regulated by insulin in hepatocytes (45). However, IRE-BP1 also decreased expression of IGFBP-3 and IGF-1, genes that are known to be stimulated by insulin (46, 47). Because therapy with adenovirus localized IRE-BP1 to the nuclei of hepatocytes or parenchymal cells (shown in Fig. 3*b*), and our prior research revealed that IGFBP-3 is synthesized by hepatic nonparenchymal cells, including Kupffer and sinusoidal endothelial cells (46), recombinant IRE-BP1 was not delivered to the cells in which IGFBP-3 synthesis normally occurs. This may account for the lack of stimulation of IGFBP-3 by IRE-BP1 when compared with up-regulation in COS-7 cells (15). We have also published previously (48) that IGF-1, as well as insulin, up-regulates IGFBP-3 mRNA. In that study, IGF-1 did not stimulate IGFBP-3 gene transcription but rather prolonged the apparent half-life of IGFBP-3 mRNA. Because our microarray studies showed that IGF-1 mRNA is decreased by IRE-BP1 overexpression (shown in Table II), the decreased IGFBP-3 mRNA level may be secondary to a decrease in mRNA stability. Decreased hepatic expression of IGF-1 may be related to effects on the coregulators reported previously for the insulin-responsive region of the gene (49) and merits further study.

To determine whether the insulin-mimetic effects of IRE-BP1 occur *in vitro*, we investigated the biological effects of IRE-BP1 in a tissue culture model. L6 cells are derived from neonatal rat thigh skeletal muscle and retain some of the properties of skeletal muscle (50). During different stages of development, these cells express the ubiquitous Glut 1 glucose transporter but not the muscle-specific Glut 4 glucose transporter (16). Glut 4 is not expressed until alignment and onset of cell fusion into myotubes (51). We found that transgenic expression of IRE-BP1 in L6 myocytes increased Glut 4 expression even without formation of multinucleated myotubes, as shown by the retention of cell morphology consistent with undifferentiated myocytes (Fig. 1, *d* and *h*). Furthermore, Glut 4 expression did not correlate with markers of differentiation, including levels of MyoD and myogenin (52, 53). Therefore, Glut 4 may be induced directly by IRE-BP1, independent of effects on cell differentiation. IRE-BP1 also increased insulin-sensitive glucose uptake, and this may be related to the expression of Glut 4 glucose transporter. Consistent with previous findings (21, 22), we found that overnight exposure of myocytes to pioglitazone increased glucose uptake significantly in L6 cells. IRE-BP1 expression increased basal glucose uptake to the same level as pioglitazone treatment, and there was no further increase in IRE-BP1-stimulated glucose transport with addition of pioglitazone, suggesting that the mechanism by which pioglitazone increases glucose uptake may converge with IRE-BP1-increased glucose uptake.

In summary, we report that the constitutive expression of IRE-BP1 in muscle cells induces changes in glucose transport and glycogen accumulation that are consistent with the involvement of IRE-BP1 in the insulin-signaling pathway regulating glucose uptake. Thus, IRE-BP1 is not only a target for phosphorylation by Akt but could potentially mediate some of the metabolic effects mediated by insulin-induced Akt signaling. IRE-BP1 is reduced in the liver with diabetes, and expression of IRE-BP1 appears to be sufficient to reduce glucose levels in diabetic rats; this is due at least in part to suppression of genes involved in gluconeogenesis, leading to decreased hepatic glucose production. Significant effects on postprandial glucose control were also observed and may be related to changes in the glycerolipid profile that may reduce circulating free fatty acids and lipid oxidation, although confirmation will require further studies. Because IRE-BP1 is distributed to all insulin target tissues (15), the mechanisms by which IRE-BP1 mediates increased sensitivity to insulin action in other organs or affects other metabolic parameters associated with the insulin resistance syndrome are appropriate topics for further study. Furthermore, studies to determine whether IRE-BP1 is not only sufficient but also necessary for the metabolic actions of insulin will be conducted. In conclusion, our study suggests that IRE-BP1 may be an important mediator of insulin action and is a promising target for the development of new therapeutic agents to help overcome insulin resistance and promote metabolic normalization in individuals with impaired glucose tolerance and type 2 diabetes.

Acknowledgments—We are grateful for the gene microarray analysis conducted by Brown Cancer Center Shared Microarray Facility (Sabina Waigel and Wolfgang Zacharias), for the thoughtful review of the manuscript by Dr. Stephen J. Winters, for the helpful suggestions of Dr. Haian Fu, and for the technical assistance of Weidong Zhao and Ying Song.

REFERENCES

1. Green, A., Christian, H. M., and Pramming, S. K. (2003) *Diabetes Metab. Res. Rev.* **19,** 3–7
2. Kruszynska, Y., and Olefsky, J. M. (1996) *J. Investig. Med.* **44,** 413–428
3. Taylor, S. I. (1999) *Cell* **97,** 9–12
4. Song, S. (2002) *Diabetes Metab. Res. Rev.* **18,** 5–12
5. Foufelle, F., and Ferre, P. (2002) *Biochem. J.* **366,** 377–391
6. Barthel, A., and Schmoll, D. (2003) *Am. J. Physiol.* **285,** E685–E692
7. Beck-Nielsen, H., Vaag, A., Poulsen, P., and Gaster, M. (2003) *Best Pract. Res. Clin. Endocrinol. Metab.* **17,** 445–467
8. Shah, P., Basu, A., and Rizza, R. (2003) *Curr. Diab. Rep.* **3,** 214–218
9. Saltiel, A. R., and Kahn, C. R. (2001) *Nature* **414,** 799–806
10. Kido, Y., Nakae, J., and Accili, D. (2001) *J. Clin. Endocrinol. Metab.* **86,** 972–979
11. Kops, J. P. L., and Burgering, B. M. T. (1999) *J. Mol. Med.* **77,** 656–665
12. Whiteman, E. L., Cho, H., and Birnbaum, M. J. (2002) *Trends Endocrinol. Metab.* **13,** 444–451
13. Altomonte, J., Richter, A., Harbaran, S., Suriawinata, J., Nakae, J., Thung, S. N., Meseck, M., Accili, D., and Dong, H. (2003) *Am. J. Physiol.* **285,** E718–E728
14. Puigserver, P., Rhee, J., Donovan, J., Walkey, C. J., Yoon, J. C., Oriente, F., Kitamura, Y., Altomonte, J., Accili, D., and Spiegelman, B. M. (2003) *Nature* **423,** 550–555
15. Villafuerte, B. C., Phillips, L. S., Rane, M. J., and Zhao, W. (2004) *J. Biol. Chem.* **279,** 36650–36659

16. Kozlovsky, N., Rudich, A., Potashnik, R., and Bashan, N. (1997) *Free Radic. Biol. Med.* **23,** 859–869
17. van der Laarse, W. J., van Noort, P., and Diegenbach, P. C. (1992) *Biotech. Histochem.* **67,** 303–308
18. Totzke, G., Sachinidis, A., and Vetter, H. (1996) *Mol. Cell. Probes* **10,** 427–433
19. Fronhoffs, S., Totzke, G., Stier, S., Werner, N., Rothe, M., Bruning, T., Koch, B., Sachinidis, A., Vetter, H., and Ko, Y. (2002) *Mol. Cell. Probes* **16,** 99–110
20. Monzillo, L. U., and Hamdy, O. (2003) *Nutr. Rev.* **61,** 397–412
21. Shin, Y., Nishimura, H., Shintani, M., Inoue, R., Yamamoto, Y., Masuzaki, H., Ogawa, Y., Hosada, K., Inoue, G., and Hayashi, T. (2001) *Diabetes Metab. Res. Rev.* **50,** 1093–1101
22. Shintani, M., Nishimura, H., Yonemitsu, S., Ogawa, Y., Hayashi, T., Hosada, K., Inoue, G., and Nakao, K. (2001) *Diabetes Metab. Res. Rev.* **50,** 2296–2300
23. Wang, Q. T., Somwar, R., Bilan, P., Liu, Z., Jin, J., Jr., and Klip, A. (1999) *Mol. Cell. Biol.* **19,** 4008–4018
24. Peterson, R. G., Shaw, W. N., Neel, M. A., Little, L. A., and Eichberg, J. (1990) *ILAR News* **32,** 16–19
25. O'Brien, R. M., and Granner, D. K. (1996) *Rev. Physiol.* **76,** 1109–1161
26. Hall, R. K., and Granner, D. K. (1999) *J. Basic Clin. Physiol. Pharmacol.* **10,** 119–133
27. Rossetti, L., Giaccari, A., Barzilai, N., Howard, K., Sebel, G., and Hu, M. (1993) *J. Clin. Investig.* **92,** 1126–1134
28. Postic, C., Shiota, M., Niswender, K. D., Jetton, T. L., Chen, Y., Moates, J. M., Shelton, K. D., Lindner, J., Cherrington, A. D., and Magnuson, M. A. (1999) *J. Biol. Chem.* **274,** 305–315
29. Polson, D. A., and Thompson, M. P. (2003) *Biochem. Biophys. Res. Commun.* **301,** 261–266
30. Baulande, S., Lasnier, F., Lucas, M., and Pairault, J. (2001) *J. Biol. Chem.* **276,** 33336–33344
31. Hermsdorf, T., and Dettmer, D. (1998) *Cell. Signal.* **10,** 629–635
32. O'Doherty, R. M., Anderson, P. R., Zhao, A. Z., Bornfeldt, K. E., and Newgard, C. B. (1999) *Am. J. Physiol.* **277,** E544–E550
33. Marchmont, R. J., and Houslay, M. D. (1980) *Nature* **286,** 904–906
34. Yamatani, K., Saito, K., Takahashi, K., Ohnuma, H., Manaka, H., and Sasaki, H. (2001) *Regul. Pept.* **99,** 45–52
35. Manganiello, V. C., Degerman, E., Taira, M., Kono, T., and Belfrage, P. (1996) *Curr. Top. Cell. Regul.* **34,** 63–100
36. Rhee, J., Inoue, Y., Yoon, J. C., Puigserver, P., Fan, M., Gonzalez, F. J., and Spiegelman, B. M. (2003) *Proc. Natl. Acad. Sci. U. S. A.* **100,** 4012–4017
37. Poirier, M., Vincent, G., Reszko, A. E., Bouchard, B., Kelleher, J. K., Brunengraber, H., and Des Rosiers, C. (2002) *Am. J. Physiol.* **283,** H1379–H1386
38. Nakamura, M. T., and Nara, T. Y. (2002) *Biochem. Soc. Trans.* **30,** 1076–1079
39. Mead, J. R., Irvine, S. A., and Ramji, D. P. (2002) *J. Mol. Med.* **80,** 753–769
40. Zammit, V. A. (1999) *Biochem. J.* **343,** 505–515
41. Louet, J. F., Le May, C., Pegorier, J. P., Decaux, J. F., and Girard, J. (2001) *Biochem. Soc. Trans.* **29,** 310–316
42. Lam, T. K., Carpentier, A., Lewis, G. F., van de Werve, G., Fantus, I. G., and Giacca, A. (2003) *Am. J. Physiol.* **284,** E863–E873
43. Boden, G. (2002) *Curr. Opin. Clin. Nutr. Metab. Care* **5,** 545–549
44. Kraegen, E. W., Cooney, G. J., Ye, J., and Thompson, A. L. (2001) *Exp. Clin. Endocrinol. Diabetes* **109,** S516–S526
45. Villafuerte, B. C., Goldstein, S., Murphy, L. J., and Phillips, L. S. (1991) *Diabetes* **40,** 837–841
46. Villafuerte, B. C., Koop, B. L., Birdsong, G. G., and Phillips, L. S. (1994) *Endocrinology* **134,** 2044–2050
47. Zhu, J. L., Pao, C. I., Hunter, E. J., Lin, K. W., Wu, G. J., and Phillips, L. S. (1999) *Endocrinology* **140,** 4761–4771
48. Villafuerte, B. C., Zhang, W., and Phillips, L. S. (1996) *Mol. Endocrinol.* **10,** 622–630
49. Kaytor, E. N., Zhu, J. L., Pao, C. I., and Phillips, L. S. (2001) *Endocrinology* **142,** 1041–1049
50. Turo, K. A., and Florini, J. R. (1982) *Am. J. Physiol.* **243,** C278–C284
51. Niu, W., Huang, C., Nawaz, Z., Levy, M., Somwar, R., Li, D., Bilan, P. J., and Klip, A. (2003) *J. Biol. Chem.* **278,** 17953–17962
52. Lu, H., Shah, P., Ennis, D., Shinder, G., Sap, J., Le-Tien, H., and Fantus, I. G. (2002) *J. Biol. Chem.* **277,** 46687–46695
53. Carnac, G., Albagli-Curiel, O., Levin, A., and Bonnieu, A. (1993) *Endocrinology* **133,** 2171–2176